

See discussions, stats, and author profiles for this publication at: <https://www.researchgate.net/publication/280392785>

Oxidative Stress Mechanisms Do Not Discriminate between Genotoxic and Nongenotoxic Liver Carcinogens

ARTICLE in CHEMICAL RESEARCH IN TOXICOLOGY · JULY 2015

Impact Factor: 3.53 · DOI: 10.1021/acs.chemrestox.5b00222 · Source: PubMed

READS

44

5 AUTHORS, INCLUDING:



Jarno Wolters

Maastricht University

2 PUBLICATIONS 1 CITATION

SEE PROFILE



Sandra M H Claessen

Maastricht University

40 PUBLICATIONS 645 CITATIONS

SEE PROFILE



Jos Kleinjans

Maastricht University

348 PUBLICATIONS 6,469 CITATIONS

SEE PROFILE

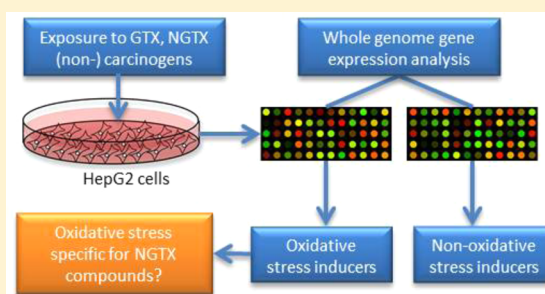
Oxidative Stress Mechanisms Do Not Discriminate between Genotoxic and Nongenotoxic Liver Carcinogens

Lize Deferme, Jarno Wolters, Sandra Claessen, Jacco Briedé,* and Jos Kleinjans

Department of Toxicogenomics, School of Oncology and Developmental Biology (GROW), Maastricht University, 6200 MD Maastricht, The Netherlands

Supporting Information

ABSTRACT: It is widely accepted that in chemical carcinogenesis different modes-of-action exist, e.g., genotoxic (GTX) versus nongenotoxic (NGTX) carcinogenesis. In this context, it has been suggested that oxidative stress response pathways are typical for NGTX carcinogenesis. To evaluate this, we examined oxidative stress-related changes in gene expression, cell cycle distribution, and (oxidative) DNA damage in human hepatoma cells (HepG2) exposed to GTX-, NGTX-, and noncarcinogens, at multiple time points (4–8–24–48–72 h). Two GTX (azathiopine (AZA) and furan) and two NGTX (tetradecanoyl-phorbol-acetate, (TPA) and tetrachloroethylene (TCE)) carcinogens as well as two noncarcinogens (diazinon (DZN, D-mannitol (Dman)) were selected, while per class one compound was deemed to induce oxidative stress and the other not. Oxidative stressors AZA, TPA, and DZN induced a 10-fold higher number of gene expression changes over time compared to those of furan, TCE, or Dman treatment. Genes commonly expressed among AZA, TPA, and DZN were specifically involved in oxidative stress, DNA damage, and immune responses. However, differences in gene expression between GTX and NGTX carcinogens did not correlate to oxidative stress or DNA damage but could instead be assigned to compound-specific characteristics. This conclusion was underlined by results from functional readouts on ROS formation and (oxidative) DNA damage. Therefore, oxidative stress may represent the underlying cause for increased risk of liver toxicity and even carcinogenesis; however, it does not discriminate between GTX and NGTX carcinogens.



INTRODUCTION

Hepatic carcinogenesis is associated with a range of risk factors but underlying mechanisms-of-action tend to be complicated and to date are not fully understood. Hepatocellular carcinoma (HCC) is the most common type of primary liver cancer worldwide and evolves from different genetic lesions at regulatory sites.¹ However, causal factors of hepatocellular carcinoma mainly originate from the environment rather than from specific genetically inherited gene mutations.² Hepatitis B and C are still considered the major risk factors for HCC (70–80%) and have thus been extensively studied.^{3,4} Also, exposure of the liver to chemicals and drugs may induce HCC.⁵ On the basis of the mode of action by which these compounds induce hepatocarcinogenesis, they are generally classified as either genotoxic (GTX) or nongenotoxic (NGTX) carcinogens.⁶ However, insights into mechanisms involved in NGTX carcinogenesis are considerably less advanced than those for GTX carcinogens.⁷

One molecular factor considered important in liver carcinogenesis is the formation of reactive oxygen species (ROS).^{5,8} Compounds may induce oxidative stress by forming reactive oxygen species (ROS) directly, by increasing endogenous cellular generation of ROS, for instance by upregulating enzymatic metabolism, or by decreasing antioxidant mechanisms. Where there is consensus that GTX carcinogens act by

directly damaging DNA and that oxidative stress is of less or even no importance for this type of carcinogens, based on evaluations of transcriptomic changes induced in the liver of rats exposed to a range of carcinogens it was suggested that the induction of oxidative stress is a typical feature of NGTX carcinogenesis.^{7,9,10} Enzyme systems such as the NADPH-oxidase complex, cyclooxygenase, xanthine-oxidase, lipoxygenase, cytochrome-P450, and peroxisomes, as well as inflammatory cells, are sources of endogenous ROS^{5,11} which may be affected by NGTX carcinogens. Upon exposure to NGTX carcinogens, intracellular accumulation of ROS from endogenous and exogenous sources that is not counteracted by antioxidants such as superoxide dismutase, catalase, or other phase II genes activated by nuclear factor (erythroid-derived 2)-like 2 (NRF2) may result in oxidative stress.

In a previous global transcriptomic study using a human hepatoma cell line (HepG2 cells), we identified a signature of 17 upregulated genes after exposure to different types of oxygen radicals.¹² As most of these genes are involved in hepatocarcinogenesis and/or oxidative stress, it is of interest to investigate the relationship between the upregulation of these genes and oxidative stress induced by NGTX carcinogens in comparison

Received: May 27, 2015

to GTX carcinogens. Consequently, for the present study, compounds were selected with regard to their ability to induce oxidative stress based on data on the expression of these genes obtained from a whole genome gene expression database generated from HepG2 cells exposed to 62 chemicals that were either classified as GTX or NGTX compounds.¹³

HepG2 cells were used as an *in vitro* model for the liver, the most important target for reactive metabolites from chemical carcinogens. Results obtained from noncancer type of liver cells or much more complex multicellular organs and *in vivo* exposure will only partially overlap with results obtained in HepG2 cells, but their ability to metabolize xenobiotics,¹⁴ although with a lower metabolic capacity compared to that of primary hepatocytes,¹⁵ the absence of p53 mutations,¹⁶ and the ease with which they can be cultured including high reproducibility in responses without interindividual variation in comparison to, for example, primary human hepatocytes, make these cells useful as a practical first screening alternative for *in vivo* testing of, e.g., GTX and NGTX compounds.¹³

For this study, two GTX carcinogens, two NGTX carcinogens, and two noncarcinogens were selected, within each class one compound inducing upregulation of genes from this oxidative stress-related gene set and the other not. Since presumably, differences in the kinetics of ROS formation exist, temporal cellular changes induced by GTX and NGTX carcinogens and noncarcinogens were analyzed at five different exposure times: 4 h, 8 h, 24 h, 48 h, and 72 h in HepG2 cells. ROS generating capacities of these compounds were measured using electron spin resonance (ESR) spectroscopy. Significantly induced molecular pathways were correlated with functional effects, e.g., ROS levels, (oxidative) DNA damage, and cell cycle progression.

MATERIALS AND METHODS

Compound Selection. Oxidative stress or nonoxidative stress-inducing GTX-, NGTX-, and noncarcinogens, as classified *in vitro* and *in vivo* using different criteria based on results from the Ames mutagenicity test, micronuclei test, chromosomal aberration test, mouse lymphoma assays, and gene classifiers specific for genotoxicity as described before,¹³ were selected based on their gene expression profile indicative for inducing oxidative stress. This selection was based on a previously published gene-set of 17 genes (BIK, AKR1C2, GCLC, GCLM, GSR, LIF, RAP1GAP, SQSTM1, GCNT3, RRAS2, SLC7A11, ASF1A, ASKRIB10, FBXO30, AGPAT9, SRXN1, and PTGR1) related to oxidative stress in HepG2 cells without taking into account prior knowledge of oxidative stress capacities of these compounds.¹² The expression of these 17 genes was evaluated using previously obtained transcriptomics data of HepG2 cells treated for 24 h and 48 h,^{13,17} with the 62 compounds present in this data set. When genes from this set showed an absolute average fold change in expression level >1.2 and a *p*-value <0.05, this gene was defined as differentially expressed. The total number of differentially expressed genes from this set was scored, and percentages were calculated for each individual compound compared to the total number of selected genes (Table S1, [Supporting Information](#)). Within the different classes of carcinogens,¹³ as well as for the noncarcinogens, an oxidative gene set-inducing compound (highest %) and a nonoxidative gene set-inducing compound (0%) were selected (Table S2, [Supporting Information](#)). This selection process resulted in six compounds; (1) azathioprine (AZA, 88%, oxidative stress inducer) and furan (0%) as GTX carcinogens, (2) tetradecanoyl phorbol acetate (TPA, 44%, oxidative stress inducer) and tetrachloroethylene (TCE, 0%) as NGTX carcinogens, and (3) diazinon (DZN, 63%, oxidative stress inducer) and D-mannitol (Dman, 0%) as noncarcinogens.

Cell Culture and Treatment. HepG2 cells (passage number #14–17, ATCC, LGC logistics) were cultured in six-well plates and 35 × 10 mm dishes in the presence of 2 mL of minimal essential medium

(MEM) plus GlutaMAX supplemented with 1% nonessential amino acids (NEAA), 1% sodium-pyruvate, 1% penicillin/streptomycin, and 10% fetal calf serum (FCS) (all from Gibco BRL, Breda, The Netherlands). The cells were incubated at 37 °C with 5% CO₂. When obtaining 80% confluence, the medium was replaced by medium containing the test compounds at the IC₂₀ concentration (= 80% viability) as derived from the MTT (3-(4,5-dimethylthiazol-2-yl)-2,5-diphenyltetrazolium bromide) cytotoxicity test at 72 h.¹³ This procedure for concentration selection is based on the hypothesis that by selecting a dose that gives a slight cytotoxic response after a relatively long incubation period of 72 h will most likely induce relevant gene expression under noncytotoxic conditions on earlier time points. Used concentrations were 250 μM AZA (dissolved in DMSO, Sigma-Aldrich), 2 mM furan (dissolved in DMSO, Sigma-Aldrich), 500 nM TPA (dissolved in DMSO, Sigma-Aldrich), 2 mM TCE (dissolved in EtOH, Sigma-Aldrich), 250 μM DZN (dissolved in DMSO, Sigma-Aldrich), and 250 μM Dman (dissolved in HBSS, Sigma-Aldrich) or with the corresponding control treatment (0.5% of DMSO, EtOH, or HBSS). Time-matched control cells were treated in an identical manner without addition of a compound.

Identification and Levels of Radical Formation. Radical formation in HepG2 cells was measured after 0.5, 2, 4, 8, 24, 48, and 72 h exposure to AZA, furan, TPA, TCE, DZN, and Dman using electron spin resonance (ESR) spectroscopy in combination with the spin probing technique using 250 μM 1-hydroxy-3-carboxy-2,2,5,5-tetramethylpyrrolidine (CPH, Noxygen, Elzach, Germany) which forms CP radicals in the presence of ROS. As a positive control, cells were exposed to 100 μM menadione (Men). CPH was added to the control and exposed cells 0.5 h prior to measurements where the triple-line spectrum of the CP radical was detected by ESR spectroscopy.¹⁸ Instrument settings were 50 mW of microwave power, 1 G of amplitude modulation, 100 kHz of modulation frequency, magnetic field of 3500 G, and 60 G sweep widths with a number of 10 scans/sample. Spectra were quantified (in arbitrary units) through peak surface measurements of the triple peak spectra of CPH (AUC = area under the curve) using the WIN-EPR spectrum manipulation program.¹⁸

Cell Cycle Distribution, Double-Strand Breaks, and Oxidative DNA Damage. Methanol-fixed cells were labeled for double strand breaks using γH2AX staining as has previously been described.¹⁹ As positive and negative controls, cells were incubated with 5 μM etoposide (Eto, Sigma-Aldrich) or the corresponding solvent controls.²⁰

For assessing 8-hydroxy-2'-deoxyguanosine (8-OHdG), the Oxy-FLow DNA-damage kit (Calbiochem, USA) was applied as described in the manufacturer's protocol. Using this method, oxidative DNA damage can be detected in cell suspension using flow cytometry. Methanol-fixed cells were incubated for 1 h with the FITC-labeled anti-8-OHdG antibody diluted 1:30 in wash solution. The antibody is in this way able to enter the cells and binds to 8-OHdG adducts produced as a result of oxidative DNA damage. After incubation, the cells were washed, resuspended in buffer, and analyzed by flow cytometry. As positive and negative controls, cells were incubated with 5 μM Eto or the corresponding solvent controls.

Cell cycle distribution was measured simultaneously using propidium iodide (PI) staining as previously described.²¹ Cell cycle, γH2AX signals, and 8-OHdG signals were analyzed using ModFit LT for Mac (version 2.0). Cells in the G1, S, or G2/M phase were expressed as a percentage of the total number of cells (10000 cells/sample). Cells with significant levels of γH2AX and 8-OHdG positive signals were presented as a percentage of total cells.

Total RNA Isolation and Microarray Experiments. Total RNA was extracted from HepG2 cells exposed to the compounds for 4, 8, 24, 48, and 72 h using 0.5 mL of QIAzol (Qiagen, Venlo, The Netherlands) according to the manufacturer's instructions. Selection of this exposure times for transcriptomics was partly based on existing transcriptomics datasets for 24 and 48 h.¹³ This dataset was extended with transcriptomics data for earlier and later exposure times with a maximum of 72 h, based on an early significant expression of genes and phenotypical responses for oxidative DNA damage.¹² RNA quality was assessed by automated gel electrophoresis on an Agilent 2100 bioanalyzer (Agilent Technologies, Amstelveen, The Netherlands).

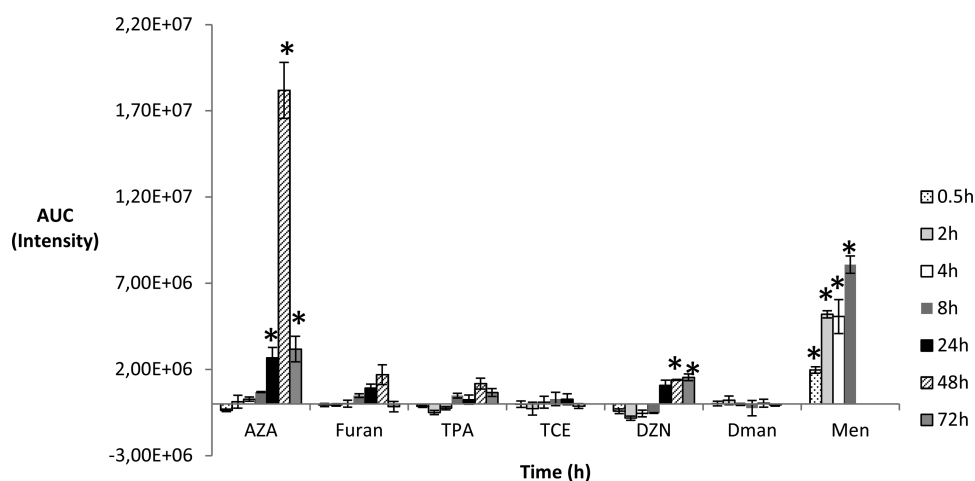


Figure 1. Levels of time dependent radical formation after exposure to AZA, furan, TPA, TCE, DZN, Dman, and Men (positive control) using ESR in combination with spin trapping by CPH. Results are corrected for background levels observed in control conditions ($n = 3$, $p < 0.05$). AUC: area under the curve of radical specific signals; t, time (h).

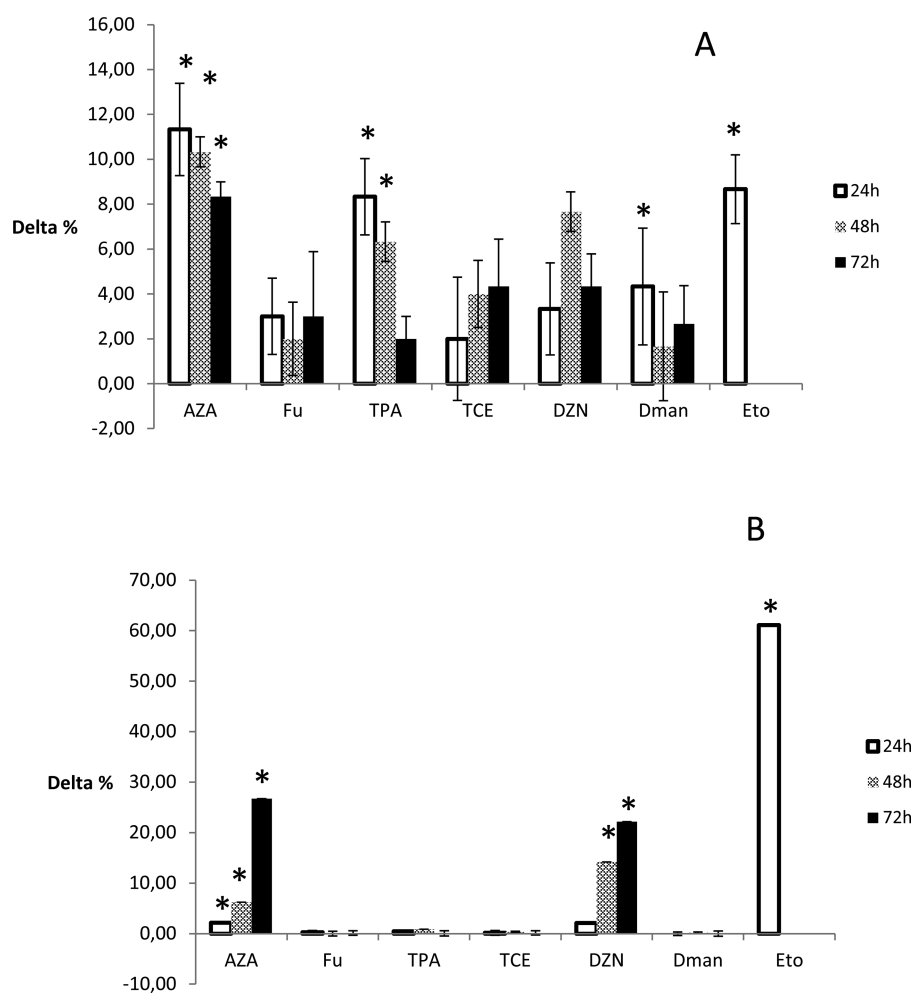


Figure 2. DNA damage induced by AZA, furan, TPA, TCE, DZN, Dman, and Eto (positive control) using flow cytometry. (A) Levels of 8-OHdG after 24, 48, and 72 h exposure. (B) Levels of γ H2AX after 24, 48, and 72 h exposure. Values were corrected for blank levels ($n = 3$, $p < 0.05$).

cDNA was prepared using Affymetrix synthesis and labeling kits as described before (Affymetrix, Santa Clara).¹⁴ cRNA targets were hybridized on high-density oligonucleotide gene-titan chips (Affymetrix Human Genome U133 Plus PM GeneTitan 24 arrays) according to the Affymetrix Eukaryotic Target Hybridization manual. The Gene-Titan arrays were hybridized, washed, and stained using the Gene-Titan

hybridization, wash, and staining kit for 3' IVT Arrays and Gene-Titan Operating Software, and scanned by means of an Affymetrix Gene-Titan scanner. Normalization quality controls, including scaling factors, average intensities, present calls, background intensities, noise, and raw Q values, were within acceptable limits for all arrays (Normalization unscaled standard errors < 1.1 , relative log expression around 0).

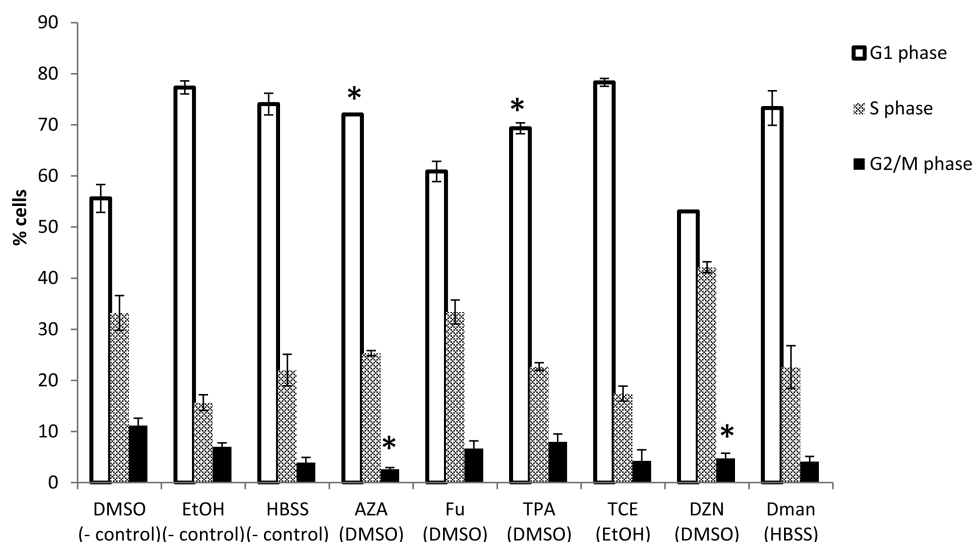


Figure 3. Levels of different cell cycle phases: G1 phase, S phase, and G2/M phase distribution after 72 h of AZA, furan, TPA, TCE, DZN, and Dman exposure in HepG2 cells using flow cytometry ($n = 3$, $p < 0.05$).

Whole Genome Gene Expression Analysis. Reannotation and Normalization. Data from a total of 135 arrays were obtained, and robust multiarray average (RMA) normalized and reannotated to custom Chip Definition Files (CDF, version 14.1.0) files using the Arrayanalysis tool (<http://arrayanalysis.org>). In addition, after correcting for platform probes, 17143 genes were analyzed for the number of absence calls in the three replicates per treatment. Genes that contained two or more absence calls within the three replicates for all the treatments as well as in controls were omitted from the data. The data discussed in this publication have been deposited in NCBI's gene expression omnibus²² and are accessible through GEO series accession number GSE58235: <http://www.ncbi.nlm.nih.gov/geo/query/acc.cgi?acc=GSE58235>.

Data Filtering. The average intensities of the three replicates of the filtered datasets were obtained, and subsequently, log ratios of treated versus controls were calculated. DEGs for each experimental group were selected using the following criteria: (1) log ratio of -0.26 or >0.26 (i.e., absolute fold change of 1.2) for the average of the three replicates within the experimental group, (2) the same direction of the log ratio for all replicates, (3) the intensity of log 2 values >6 for at least 2 out of 3 replicates, and (4) a p value of <0.05 determined using Student's t test.

Pathway Analysis of DEGs. MetaCore (GeneGo, San Diego, CA) was used to identify and visualize the involvement of the DEGs and transcription factors in the biological processes that may be affected at the level of pathways, by selecting significant pathways with a p value <0.05 .

Time Series Analyses by STEM. For the identification of genes coregulated time-dependently and clustering with markers for oxidative stress, the software tool "Short Time-series Expression Miner" (STEM 1.3.8; <http://www.cs.cmu.edu/~jernst/stem/>)²³ was used. The criteria used were described before.²⁴

Statistical Analysis. Data for all experiments were gathered in triplicate and are presented as the means \pm SEM. Statistical analyses of changes, for each time point compared to that of the control, were performed using an unpaired two-tailed Student's t test (in levels of radical formation) or a paired two-tailed Student's t test (in (oxidative) DNA-damage and cell cycle distributions) with statistical significance set at $p < 0.05$.

For correlation analysis between gene expression and functional end points (γ H2AX, 8-oxodG, and cell cycle distribution levels), all data were transformed into log 2 ratios and correlated to significant ($p < 0.05$) time profiles using STEM.

RESULTS

Detection of ROS Formation and Functional Effects.

ROS Formation after Exposure to Selected Compounds. In the presence of HepG2 cells and the spin probe CPH, AZA exposure for 24, 48, and 72 h, as well as DZN exposure at 48 and 72 h, resulted in significantly increased levels of cellular ROS production (Figure 1). TPA, however, did not induce a significant increase of ROS levels. As expected, the nonoxidative stress-inducing compounds TCE, furan, and Dman did not cause ROS formation. On the basis of these results, the following incubation periods were selected for further studies on (oxidative) DNA damage and cell cycle distribution: 8, 24, 48, and 72 h. And in addition, whole genome gene expression was also evaluated after 4 h of exposure.

(Oxidative) DNA Damage after Carcinogen Exposure. AZA, as well as the noncarcinogen, DZN, induced a significant increase in 8-OHdG and γ H2AX signals after 24, 48, and 72 h (Figure 2A and B; see for examples of FACS histograms, Figure S1, Supporting Information), except for DZN at 24 h. Twenty-four and 48 h TPA treatment resulted in a significantly elevated signal of 8-OHdG adducts (Figure 2A) but not of ROS levels (Figure 1). However, none of these compounds induced (oxidative) DNA damage after 8h exposure (data not shown). Exposure to furan, TCE, or Dman did not result in a significant increase in (oxidative) DNA damage over time (Figure 2A and B). Overall, our findings show that the selected oxidative stress-inducing compounds, AZA and DZN, are able to cause (oxidative) DNA damage and ROS formation while the nongenotoxic oxidative stress-inducer TPA is only able to cause a significant increase in oxidative DNA damage.

Cell Cycle Distribution after Carcinogen Exposure. With regard to cell cycle changes, 48 h (data not shown) and 72 h (Figure 3) of AZA exposure (see for examples of FACS histograms Figure S2, Supporting Information) and 24 h of furan treatment (data not shown) resulted in a significant decrease in G2 phase, indicating G1/S phase arrest. TPA exposure, however, affected the cell cycle by inducing G1 phase arrest after 24, 48, and 72 h of exposure, whereas TCE treatment had no effect on cell cycle distribution. DZN exposure affected the cell cycle by simultaneously decreasing the G1 phase and increasing the S phase at 24 h (data not shown) and decreasing the G2 phase at 72

h (Figure 3) while Dman treatment induced an increase in S phase after 48 h of exposure, indicating that both DZN and Dman are capable of inducing S phase arrest in HepG2 cells. These results show that S phase arrest by these GTX- and noncarcinogens can develop without concomitant oxidative stress, whereas G1 phase arrest was specifically induced by the NGTX carcinogen TPA.

Oxidative Stress-Related Gene Expression Changes.

Overall, oxidative stress inducers, AZA (5155 DEGs), TPA (7445 DEGs), and DZN (6838 DEGs), induced a 5–10 fold higher number of DEGs compared to the nonoxidative stress inducers, furan (755 DEGs), TCE (1306 DEGs), and Dman (696 DEGs).

Common DEGs after Exposure to Oxidative Stressors.

When comparing gene expression after AZA, TPA, and DZN treatment, 3276 genes were found to be commonly modified (Figure 4A), and these could be assigned to 277 significant

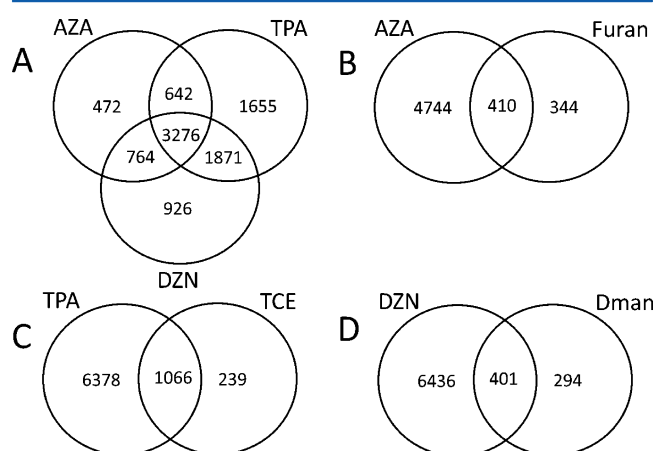


Figure 4. Venn diagrams of differentially expressed genes after exposure to (A) AZA, TPA, and DZN; (B) AZA and furan; (C) TPA and TCE; and (D) DZN and Dman over all time points showed unique and overlapping genes.

pathways in particular involved in cell cycle changes, apoptosis, DNA damage oxidative stress regulation, and immune responses (Table 1). These common DEGs include among others (in)direct oxidative stress-related genes such as NRF2, KEAP1, NF- κ B, GCLC, GCLM, GSTA4, NQO1, HMOX1, MSH6, CDKN1A, and CCND1. Unique genes referred to specific responses (Table 2) such as 25 pathways mainly involved in the cytoskeleton and developmental processes induced by AZA treatment (Table 2A). Fifty-five pathways induced by the NGTX carcinogen TPA appeared related to signal transduction, apoptosis/survival responses and developmental processes (Table 2B), while 16 pathways following DZN treatment were mainly involved in immune responses (Table 2C). Exposure to noncarcinogens, DZN and Dman, resulted in 401 common DEGs in HepG2 cells (Figure 4D) in particular involved in signal transduction and developmental pathways. Overall, the high number of DEGs commonly induced by AZA, TPA, and DZN, appeared to be involved in cell cycle-, DNA damage-, and oxidative stress-related events. These results indicate that the oxidative stress-related gene expression response is similar among the oxidative genotoxic-, nongenotoxic-, and noncarcinogens and does not seem to represent a specific event in nongenotoxic carcinogenesis.

Table 1. Selection of Most Significantly Regulated Processes and Involved Pathways Based on 3276 Common DEGs Induced by AZA, TPA, and DZN Treatment^a

pathways and cellular processes	p value
Cell Cycle and Its Regulation	
the metaphase checkpoint	5.661×10^{-12}
start of DNA replication in early S phase	3.307×10^{-10}
chromosome condensation in prometaphase	8.742×10^{-09}
DNA-Damage Response	
ATM/ATR regulation of G1/S checkpoint	2.242×10^{-07}
role of Brca1 and Brca2 in DNA repair	5.396×10^{-07}
ATM/ATR regulation of G2/M checkpoint	2.141×10^{-05}
Apoptosis	
endoplasmic reticulum stress response pathway	4.333×10^{-07}
granzyme A signaling	3.710×10^{-06}
HTR1A signaling	5.690×10^{-05}
Tissue Remodeling and Wound Repair	
TGF, WNT, and cytoskeletal remodeling	4.695×10^{-12}
MIF-induced cell adhesion, migration, and angiogenesis	2.226×10^{-08}
chemokines and adhesion	4.851×10^{-08}
Metabolic Diseases	
role of ER stress in obesity and type 2 diabetes	2.956×10^{-07}
role of adipose tissue hypoxia in obesity and type 2 diabetes	1.196×10^{-04}
Immune System Response	
IFN gamma signaling pathway	4.264×10^{-09}
oncostatin M signaling via MAPK in human cells	9.139×10^{-09}
C5a signaling	6.808×10^{-07}
Oxidative Stress Regulation	
MIF-induced cell adhesion, migration and angiogenesis	2.226×10^{-08}
IL-18 signaling	4.633×10^{-06}
glucocorticoid receptor signaling	2.990×10^{-04}
Protein Degradation	
role of parkin in the ubiquitin-proteasomal pathway	1.479×10^{-03}
putative SUMO-1 pathway	1.172×10^{-03}
Transcription Regulation	
CREB pathway	2.033×10^{-07}
role of AP-1 in regulation of cellular metabolism	9.489×10^{-05}
receptor-mediated HIF regulation	1.314×10^{-04}
Angiogenesis	
role of IL-8 in angiogenesis	6.978×10^{-08}
FGFR signaling pathway	1.280×10^{-07}
PDGF signaling via STATs and NF- κ B	1.547×10^{-06}

^aA summary of significantly ($p < 0.05$, FDR $< 5\%$) regulated pathways and related cellular processes as indicated by MetaCore is shown.

DEGs after Exposure to GTX and NGTX Carcinogens. By comparing GTX carcinogens, furan, and AZA, 410 DEGs were found to be affected by both compounds (Figure 4B). Commonly expressed genes are mainly involved in immune and developmental processes (Figure 5A). Additionally, the DNA damage-related pathways and mismatch repair were commonly changed, as well as several pathways involved in cell cycle regulation (Figure 5A). It has to be noted that apart from these pathways, a few common DEGs included among others oxidative stress-related genes such as GCLC, GCLM, HMOX1, and GSR which were upregulated upon AZA challenge but downregulated following furan treatment. Upregulation of NRF2 or specific oxidative stress-related pathways as observed following AZA challenge were not induced by furan.

NGTX carcinogens TPA and TCE affected a total of 1066 common DEGs especially involved in developmental, immune, and cell cycle processes (Figure 4C and Figure 5B). Commonly

Table 2. Selection of Most Significantly Regulated Processes and Involved Pathways Based on Unique DEGs Induced by (A) AZA, (B) TPA, and (C) DZN Treatment^a

pathways and cellular processes	p value
A. Significantly Affected Pathways after AZA Treatment	
Cytoskeleton Remodeling	
cytoskeleton remodeling	9.035×10^{-06}
TGF, WNT, and cytoskeletal remodeling	1.800×10^{-05}
FAK signaling	1.002×10^{-03}
role of activin A in cytoskeleton remodeling	2.337×10^{-03}
Development	
TGF- β -dependent induction of EMT via MAPK	3.719×10^{-05}
thromboxane A2 pathway signaling	4.737×10^{-05}
CNTF receptor signaling	8.529×10^{-05}
EGFR signaling via small GTPases	9.678×10^{-04}
B. Significantly Affected Pathways after TPA Treatment	
Signal Transduction	
activation of PKC via G-Protein coupled receptor	3.526×10^{-05}
angiotensin signaling via STATs	1.201×10^{-04}
JNK pathway	1.639×10^{-04}
regulation of p38 and JNK signaling mediated by G-proteins	5.187×10^{-04}
Apoptosis and Survival	
antiapoptotic TNFs/NF- κ B/Bcl-2 pathway	2.692×10^{-05}
BAD phosphorylation	1.639×10^{-04}
APRIL and BAFF signaling	2.619×10^{-03}
ceramides signaling pathway	3.043×10^{-03}
Development	
A3 receptor signaling	5.560×10^{-04}
G-CSF signaling	5.560×10^{-04}
TGF- β receptor signaling	6.491×10^{-04}
A2B receptor: action via G-protein α s	6.491×10^{-04}
C. Significantly Affected Pathways after DZN Treatment	
Immune System Response	
lectin induced complement pathway	2.418×10^{-06}
function of MEF2 in T lymphocytes	2.886×10^{-06}
classical complement pathway	4.061×10^{-06}
IFN γ signaling pathway	3.257×10^{-04}
alternative complement pathway	3.401×10^{-04}

^aA summary of significantly ($p < 0.05$, FDR $< 5\%$) regulated pathways and related cellular processes as indicated by MetaCore is shown.

expressed genes among others included oxidative stress-related genes such as NRF2 and catalase and different cyclin dependent

kinases (CDK), which were significantly downregulated while NF- κ B and DNA damage-related cell cycle regulator, p21, was found to be upregulated. Changes in expression of oxidative stress-related genes upon TPA challenge such as GCLC, GCLM, GSTA4, NQO1, and HMOX2 were not observed following TCE treatment.

In conclusion, oxidative and nonoxidative GTX- or NGTX carcinogens have many pathways in common, while most oxidative stress-related genes are differently induced as a function of their oxidative capacities.

Time-Related Events Induced by Different Oxidative Stress-Inducing Chemicals. Using STEM, each gene was assigned to a model profile to which its temporal gene expression profile most closely matched based on the correlation coefficient. This tool offers more insights into how coherently induced genes are involved in dynamic cellular responses to oxidative stress and compound-specific time-dependent gene expression. DEGs resulting from AZA, TPA, and DZN exposure were assigned to four, nine, and six different significant time clusters, respectively (data not shown).

Between these oxidative stress-inducing chemicals, one identical time cluster containing coregulated genes that were simultaneously downregulated over time was identified (data not shown). Moreover, 58 common DEGs out of the overlapping 3276 DEGs (Figure 4A) in this time cluster were observed to have identical expression profiles after exposure to AZA, TPA, and DZN (Table S3). Pathway analysis using MetaCore showed that most of these genes appeared to be involved in the cell cycle, DNA damage, and repair processes. In addition, DZN and AZA appeared to share 3 identical time clusters consisting of 1605 common DEGs, indicating a major resemblance of gene expression changes over time among these two chemicals. Nonoxidative stress inducers (furan, TCE, and D-man) affected a significantly smaller amount of DEGs, which were assigned to seven or more different time profiles which did not overlap with each other. This indicates that oxidative stressors induce similar response pathways over time, independently of their specific carcinogenic potential.

Phenotypical Anchoring of Oxidative Stress-Related Transcriptomic Events. Temporal gene expression changes were correlated to functional end points such as cell cycle and (oxidative) DNA damage levels over time (Figure 6) using STEM. In addition, DEGs correlating with functional parameters and coregulated in different time clusters were assigned to

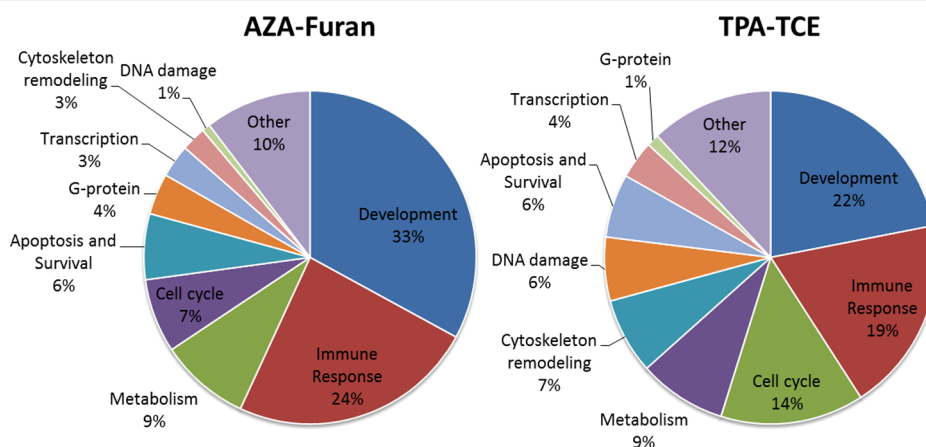


Figure 5. Pie chart representation of pathway analysis for DEGs of (A) AZA-furan and (B) TPA-TCE exposure in HepG2 cells. Pie charts show the percentage of significantly influenced cellular components with a cutoff of P -value < 0.05 ; FDR < 0.5 .

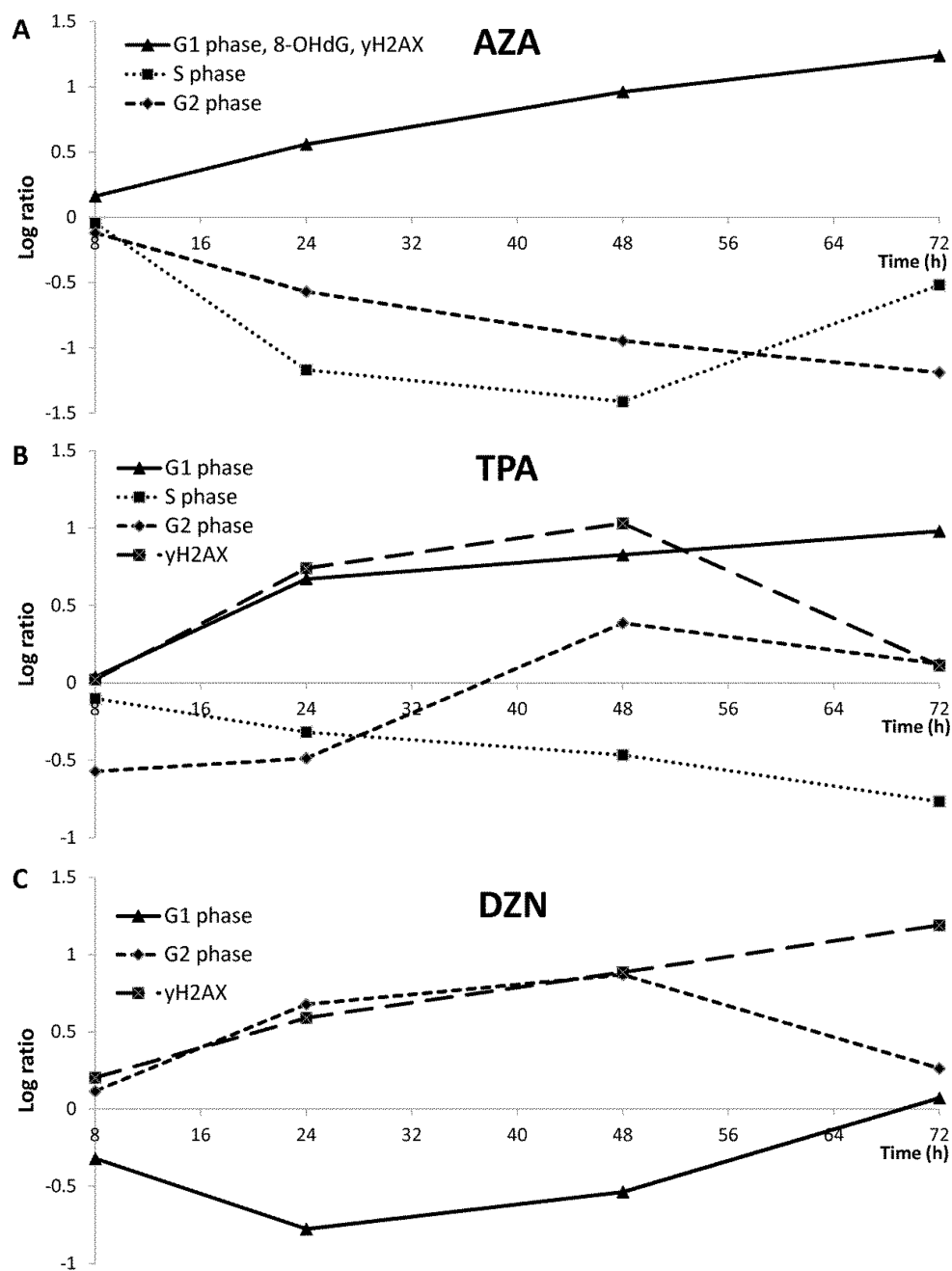


Figure 6. Average temporal gene expression correlating to levels of (oxidative) DNA damage and cell cycle distribution presented as time profiles generated by STEM after exposing HepG2 cells to (A) AZA, (B) TPA, and (C) DZN during 8, 24, 48, and 72 h.

various pathways that were identified by MetaCore. A high number of DEGs induced by AZA correlated with phenotypic end points for oxidative stress, including increased G1 phase levels, as well as 8-OHdG- and γ H2AX levels (Figure 6A). MetaCore analysis of correlating DEGs returned several pathways involved in G1/S phase transition and apoptosis, but also pathways involved in cytoskeleton, immune, and developmental processes, were observed (Table 3A). In addition, decreasing S and G2 phase levels induced by AZA over time correlated with genes involved in cell cycle- and DNA damage-related processes (Table 3A and Figure 6A). These cellular responses induced by AZA were especially affected at 24, 48, and 72 h exposure, which can be associated with significantly increased ROS levels induced by AZA at these time points. On the contrary, functional effects induced by the nonoxidative GTX

carcinogen furan did not correlate significantly with DEGs. Where TPA-induced oxidative DNA damage levels did not have any correlation with DEGs, increasing levels of G1 and G2 phases correlated with apoptotic processes, and γ H2AX levels correlated with immune responses, the cytoskeleton, and DNA damage responses such as BRCA1-regulated DNA repair (Figure 6B and Table 3B). Functional responses caused by the nonoxidative NGTX carcinogen TCE did not correlate significantly with any DEG.

Increasing G1 phase and γ H2AX levels induced by the oxidative noncarcinogen DZN over time correlated with DEGs (Figure 6C) involved in relevant cell cycle pathways and DNA damage responses but also in immune responses and apoptotic pathways (Table 3C). γ H2AX levels induced by DZN also correlated with γ H2AX levels induced by AZA. DZN-induced G2

Table 3. Genes That Clustered in the Same Gene Expression Cluster Profiles with Measured Phenotypic End Points Such as Cell Cycle and (Oxidative) DNA Damage Using STEM after (A) AZA, (B) TPA, and (C) DZN Exposure^a

A. Phenotypical Anchoring after AZA Administration			
end point	#	processes	most significant pathways
G1 phase -8-OHdG – γ H2AX	262	cell cycle	regulation of G1/S phase transition parts 1 and 2
		apoptosis	PKR in stress-induced apoptosis, activin A signaling
		DNA damage	Brca1 as a transcription regulator
		immune response	oncostatin Mn IL-2, PKR, and IL-6 signaling
		cytoskeleton	TGF, WNT, and cytoskeleton remodeling
		development	TGF β receptor signaling, EGFR signaling
S phase	21	cell cycle	metaphase checkpoint, DNA replication in early S phase, APC, and ESR1 in cell cycle regulation, chromosome condensation
G2 phase	12	cell cycle	chromosome condensation in prometphase
		protein folding	angiotensin system
B. Phenotypical Anchoring after TPA Administration			
end point	#	process	most significant pathways
G1 phase	7	apoptosis	TNF α signaling
G2 phase	4	DNA damage	Brca1 and Brca2 regulation in DNA repair
γ H2AX	35	DNA damage	Brca1 as a transcription regulator
		cytoskeleton	TGF, WNT, and cytoskeleton remodeling
		immune response	IL1, MIF and IL-12 signaling
C. Phenotypical Anchoring after DZN Administration			
end point	#	process	most significant pathways
G1 phase	35	cell cycle	start of DNA replication in early S phase, APC in cell cycle regulation, ESR1 regulation in G1/S phase transition
		DNA damage	nucleotide excision repair, Brca1, and Brca2 in DNA repair
G2 phase	7	cytoskeleton	TGF, WNT, and cytoskeleton remodeling
γ H2AX	317	DNA damage	Brca1 as a transcription regulator
		apoptosis	PKR in stress-induced apoptosis, HTR1A signaling
		immune response	oncostatin M, IFN γ signaling

*^a*Amount (#) and most significant ($p < 0.05$, FDR $< 5\%$) processes and pathways as indicated by MetaCore.

^aAmount (#) and most significant ($p < 0.05$, FDR < 5%) processes and pathways as indicated by MetaCore.

and S phase changes correlated with expression levels of multiple genes; however, these genes did not return any significant

pathways. In addition, these effects after especially 48 and 72 h of DZN exposure also were associated with significantly increased ROS formation by this compound at these time points. On the contrary, S phase changes induced by Dman correlated with DEGs, especially involved in developmental pathways and cell cycle-related pathways (data not shown).

These observations indicate that dynamic oxidative stress-related molecular events were associated with increased ROS formation. These correlations again were very similar among AZA, TPA, and DZN, and therefore, these oxidative stress-induced processes do not discriminate between GTX and NGTX carcinogens.

DISCUSSION

In this study, oxidative stress-related mechanisms in HepG2 were compared among GTX-, NGTX-, and noncarcinogens. Compounds were selected based on their capacity to induce a previously identified oxidative stress-specific gene set in HepG2¹² without using prior knowledge of oxidative stress capacities of the compounds. The presence of cellular oxidative stress induced by AZA, TPA, and DZN was confirmed by ESR spectroscopy, analysis of 8-OHdG levels, and gene expression data. These results, as summarized in Table 4, demonstrate the relevance of the previously described gene list to predict oxidative stress-inducing capacities of unknown compounds.¹² Additionally, it has been described that the development of oxidative stress, as defined earlier²⁵ as a process induced by an imbalance between oxidants and antioxidants in favor of oxidants, can be induced by AZA, TPA, and DZN.^{26–28}

Functional correlation over time showed the activation of repair and cell cycle processes simultaneously with induced (oxidative) DNA damage and cell cycle arrest by oxidative stressors AZA, TPA, and DZN. In addition, temporal oxidative stress-related events between these compounds were very similar over time, showing similar kinetics. These results indicate that oxidative stress-related mechanisms are not limited to non-genotoxic carcinogens and therefore do not discriminate between GTX and NGTX carcinogenesis.

GTX Carcinogens. GTX carcinogens, AZA and furan, need metabolic activation to exert their genotoxic characteristics. AZA is metabolized to 6-mercaptopurine by the rate-limiting enzyme thiopurine methyltransferase (TPMT),²⁹ which was found to be upregulated in our study. Furthermore, observed oxidative DNA damage and simultaneously, early G1 phase arrest indicate the activation of repair mechanisms over time as demonstrated by the induction of pathways correlated with cell cycle processes, apoptosis, and developmental processes. The involvement of oxidative stress responses in AZA-induced hepatotoxicity has been described recently.²⁸ Since interestingly, no GTX-related events were observed among pathways uniquely affected by AZA, we believe that for this compound oxidative stress is very likely an initial event related to GTX carcinogenesis.

Table 4. Overview of Effects Induced by AZA, Furan, TPA, TCE, DZN, and Dman

compd	classification	% ox. stress- related genes	ROS formation	8OHdG	γ H2AX	cell cycle	# genes
AZA	GTX carcinogen	88%	+	+	+	S phase arrest	5155
furan	GTX carcinogen	0%	–	–	–	S phase arrest	755
TPA	NGTX carcinogen	44%	–	+	–	G1 phase arrest	7445
TCE	NGTX carcinogen	0%	–	–	–	no effect	1306
DZN	noncarcinogen	63%	+	+	+	S phase arrest	6838
Dman	noncarcinogen	0%	–	–	–	S phase arrest	696

Exposure of HepG2 cells to furan did not show any DNA damage or increase in oxidative stress-regulated genes/pathways; however, the presence of an S phase arrest as well as changes in the expression of genes involved in mismatch repair indicates a response to cellular damage.

NGTX Carcinogens. NGTX carcinogen TPA, a tumor promoter, exerts its toxic effects by activation of protein kinase C (PKC) and integrins, which may lead to downstream ROS formation by NADPH oxidase activity.²⁶ Our results confirm this mechanism of action since after 24 h and 48 h of TPA treatment, PKC expression as well as its activation pathway appeared significantly upregulated. In addition, TPA-induced oxidative stress-related genes and pathways such as the NRF2 pathway, cell cycle processes, and DNA damage responses correlated with functional end points. However, the formation of oxygen radicals formed by TPA was not confirmed by ESR spectroscopy. Possibly, the downstream ROS formation is indeed capable of inducing oxidative DNA damage but amounts may be too low to be detected by ESR, or ROS formed by NADPH oxidase activity can be captured by antioxidants more effectively. NGTX carcinogens may also bind with high affinity to the aryl hydrocarbon receptor (AhR),³⁰ as demonstrated in gene expression data of TPA, where AHR expression was increased after all exposure periods.

TCE exposure induced changes in pathways involved in DNA damage and cell cycle processes, while (oxidative) DNA damage was not significantly induced. This may indicate that these pathways are not affected by stimuli of cellular damage but are deregulated indirectly by this compound, possibly by an unknown mechanism upregulating p21 expression. In addition, NF- κ B was upregulated after 8 h of exposure, while NRF2 and CAT were downregulated at that time, which was also observed after TPA exposure. Possibly, NRF2 expression is directly downregulated by NF- κ B as previously been described.³¹

The fact that mechanisms such as PKC activation by TPA lead to increased ROS formation, cell cycle-, immune-, antioxidant-, and DNA damage responses highlights that disturbance of the oxidant–antioxidant balance is a key factor in the carcinogenic events induced by the NGTX compound TPA. However, it is important to stress that temporal modifications of the NRF2 pathway, cell cycle processes, and DNA damage responses were in common between TPA and AZA, as were oxidative DNA damage and cell cycle changes. This does not subscribe to the hypothesis that the induction of oxidative stress responses is a specific event in NGTX carcinogenesis.

Noncarcinogens. The noncarcinogen DZN is metabolized by oxidative desulfuration to diazoxon which can decrease antioxidant capacities of CAT and SOD,²⁷ which was also suggested by our results. This may disturb the physiological balance between oxidants and antioxidants dramatically and can ultimately lead to oxidative stress. Consequently, NRF2, GCLC, GCLM, and other first response mechanisms against oxidative stress were found to be highly upregulated. Interestingly, these oxidative stress-related responses induced by the noncarcinogen, DZN, were similar to those after exposure to the GTX carcinogen, AZA. Both compounds induced significant ROS formation after 48 and 72 h; however, ROS levels were much higher after AZA treatment. γ H2AX levels were similarly induced by both AZA and DZN. Furthermore, both AZA and DZN exposure induced a large number of coherent processes that were similar over time and comprised DNA damage responses, cell cycle processes, immune responses, apoptotic/survival processes

and cellular development. It thus seems that, DZN possesses some GTX characteristics *in vitro* induced by oxidative stress.

Conclusions. All ROS-forming compounds investigated in the present study induced oxidative DNA damage and shared a significant number of DEGs and temporal gene expression patterns especially involved in oxidative stress-related processes such as antioxidant functions, DNA damage, cell cycle changes, and immune responses as well as specific oxidative stress regulation processes. Differences in gene expression between these compounds, however, did not directly correlate to oxidative stress, DNA damage, or cell cycle processes but could instead be assigned to compound-specific characteristics. In general, these results suggest that oxidative stress does not discriminate between GTX and NGTX carcinogens but instead represent generic responses to the compound's oxidative metabolism. Moreover, cellular oxidative stress has a strong pronounced temporal effect on DNA damage, gene expression, and cell cycle distribution for certain compounds. We state that oxidative stress still may very well represent the underlying mechanism for increased risk of liver toxicity and carcinogenesis, although follow-up studies will be necessary to complement omics-type data with phenotypical measurements by using, e.g., primary human hepatocytes and *in vivo* experiments, to confirm this. An overview of toxicogenomics approaches applied to other genotoxic and nongenotoxic liver carcinogens was provided earlier.³² Complementary to this, we here demonstrated the eminent role of oxidative stress in chemical carcinogenesis. This is supported by the fact that ROS play a major role in the carcinogenicity induced by other types of chemicals,³³ as well as the fact that increased levels of superoxide anions are involved in the modulation of risk factors for HCC.³⁴ Furthermore, oxidative stress levels have also been shown to be indicative of the success of treatment of HCC patients.³⁵

■ ASSOCIATED CONTENT

§ Supporting Information

The Supporting Information is available free of charge on the ACS Publications website at DOI: [10.1021/acs.chemrestox.5b00222](https://doi.org/10.1021/acs.chemrestox.5b00222).

Typical examples of a FACS histogram for γ H2AX determination in HepG2 cells after DMSO and AZA exposure for 72 h; typical example of a FACS histogram for cell cycle determination in HepG2 cells after DMSO or AZA exposure for 72 h; percentages of the scored up-arrows were calculated for each individual compound compared to the total amount of selected genes for genotoxic carcinogens, nongenotoxic and noncarcinogens; compound selection based on 24 h exposure to different compounds and scored for selected genes; and 58 DEGs assigned to the common time cluster observed in all oxidative stress inducing chemicals (PDF)

■ AUTHOR INFORMATION

Corresponding Author

*Department of Toxicogenomics, Faculty of Health, Medicine and Life Sciences, Maastricht University, Universiteitssingel 50, 6229 ER Maastricht, The Netherlands. Phone: +31 43 3881094. Fax: +31 43 3884146. E-mail: j.briede@maastrichtuniversity.nl.

Notes

The authors declare no competing financial interest.

■ ABBREVIATIONS

AZA, azathioprine; CPH, 1-hydroxy-3-carboxy-2,2,5,5-tetramethylpyrrolidine; 8-OHdG, 8-oxo-deoxyguanosine; CDF, chip definition files; DZN, diazinon; DEGs, differentially expressed genes; Dman, D-mannitol; ESR, electron spin resonance; Eto, etoposide; GTX, genotoxic; GSH, glutathione; HCC, hepatocellular carcinoma; H₂O₂, hydrogen peroxide; Men, menadione; NGTX, non-genotoxic; PI, propidium-iodide; ROS, reactive oxygen species; RMA, robust multiarray average; STEM, Short Time-series Expression Miner; TCE, tetrachloroethylene; TPA, tetradecanoyl phorbol acetate

■ REFERENCES

- (1) Bruix, J., Boix, L., Sala, M., and Llovet, J. M. (2004) Focus on hepatocellular carcinoma. *Cancer Cell* 5, 215–219.
- (2) Aravalli, R. N., Cressman, E. N., and Steer, C. J. (2013) Cellular and molecular mechanisms of hepatocellular carcinoma: an update. *Arch. Toxicol.* 87, 227–247.
- (3) Marra, M., Sordelli, I. M., Lombardi, A., Lamberti, M., Tarantino, L., Giudice, A., Stiuso, P., Abbruzzese, A., Sperlongano, R., Accardo, M., Agresti, M., Caraglia, M., and Sperlongano, P. (2011) Molecular targets and oxidative stress biomarkers in hepatocellular carcinoma: an overview. *J. Transl. Med.* 9, 171.
- (4) Shlomai, A., de Jong, Y. P., and Rice, C. M. (2014) Virus associated malignancies: The role of viral hepatitis in hepatocellular carcinoma. *Semin. Cancer Biol.* 26, 78–88.
- (5) Klaunig, J. E., Wang, Z., Pu, X., and Zhou, S. (2011) Oxidative stress and oxidative damage in chemical carcinogenesis. *Toxicol. Appl. Pharmacol.* 254, 86–99.
- (6) Oliveira, P. A., Colaco, A., Chaves, R., Guedes-Pinto, H., De-La-Cruz, P. L., and Lopes, C. (2007) Chemical carcinogenesis. *An. Acad. Bras. Cienc.* 79, 593–616.
- (7) Ellinger-Ziegelbauer, H., Stuart, B., Wahle, B., Bomann, W., and Ahr, H. J. (2005) Comparison of the expression profiles induced by genotoxic and nongenotoxic carcinogens in rat liver. *Mutat. Res., Fundam. Mol. Mech. Mutagen.* 575, 61–84.
- (8) Beddowes, E. J., Faux, S. P., and Chipman, J. K. (2003) Chloroform, carbon tetrachloride and glutathione depletion induce secondary genotoxicity in liver cells via oxidative stress. *Toxicology* 187, 101–115.
- (9) Fielden, M. R., Adai, A., Dunn, R. T., II, Olaharski, A., Searfoss, G., Sina, J., Aubrecht, J., Boitier, E., Nioi, P., Auerbach, S., Jacobson-Kram, D., Raghavan, N., Yang, Y., Kincaid, A., Sherlock, J., Chen, S. J., Car, B., and Predictive Safety Testing Consortium, C. W. G. (2011) Development and evaluation of a genomic signature for the prediction and mechanistic assessment of nongenotoxic hepatocarcinogens in the rat. *Toxicol. Sci.* 124, 54–74.10.1093/toxsci/kfr202
- (10) Tasaki, M., Umemura, T., Suzuki, Y., Hibi, D., Inoue, T., Okamura, T., Ishii, Y., Maruyama, S., Nohmi, T., and Nishikawa, A. (2010) Oxidative DNA damage and reporter gene mutation in the livers of gpt delta rats given non-genotoxic hepatocarcinogens with cytochrome P450-inducible potency. *Cancer Sci.* 101, 2525–2530.
- (11) Finkel, T. (2003) Oxidant signals and oxidative stress. *Curr. Opin. Cell Biol.* 15, 247–254.
- (12) Deferme, L., Briede, J. J., Claessen, S. M., Jennen, D. G., Cavill, R., and Kleinjans, J. C. (2013) Time series analysis of oxidative stress response patterns in HepG2: A toxicogenomics approach. *Toxicology* 306, 24–34.
- (13) Magkouloupoulou, C., Claessen, S. M., Tsamou, M., Jennen, D. G., Kleinjans, J. C., and van Delft, J. H. (2012) A transcriptomics-based in vitro assay for predicting chemical genotoxicity in vivo. *Carcinogenesis* 33, 1421–1429.
- (14) Jennen, D. G., Magkouloupoulou, C., Ketelslegers, H. B., van Herwijnen, M. H., Kleinjans, J. C., and van Delft, J. H. (2010) Comparison of HepG2 and HepaRG by whole-genome gene expression analysis for the purpose of chemical hazard identification. *Toxicol. Sci.* 115, 66–79.
- (15) Gerets, H. H., Tilmant, K., Gerin, B., Chanteux, H., Depelchin, B. O., Dhalluin, S., and Atienzar, F. A. (2012) Characterization of primary human hepatocytes, HepG2 cells, and HepaRG cells at the mRNA level and CYP activity in response to inducers and their predictivity for the detection of human hepatotoxins. *Cell Biol. Toxicol.* 28, 69–87.
- (16) Hsu, I. C., Tokiwa, T., Bennett, W., Metcalf, R. A., Welsh, J. A., Sun, T., and Harris, C. C. (1993) p53 gene mutation and integrated hepatitis B viral DNA sequences in human liver cancer cell lines. *Carcinogenesis* 14, 987–992.
- (17) Allen, S. A., Clark, W., McCaffery, J. M., Cai, Z., Lanctot, A., Slininger, P. J., Liu, Z. L., and Gorsich, S. W. (2010) Furfural induces reactive oxygen species accumulation and cellular damage in *Saccharomyces cerevisiae*. *Biotechnol. Biofuels* 3, 2.
- (18) Briede, J. J., De Kok, T. M., Hogervorst, J. G., Moonen, E. J., Op Den Camp, C. L., and Kleinjans, J. C. (2005) Development and application of an electron spin resonance spectrometry method for the determination of oxygen free radical formation by particulate matter. *Environ. Sci. Technol.* 39, 8420–8426.
- (19) Magkouloupoulou, C., Claessen, S. M., Jennen, D. G., Kleinjans, J. C., and van Delft, J. H. (2011) Comparison of phenotypic and transcriptomic effects of false-positive genotoxins, true genotoxins and non-genotoxins using HepG2 cells. *Mutagenesis* 26, 593–604.
- (20) Watters, G. P., Smart, D. J., Harvey, J. S., and Austin, C. A. (2009) H2AX phosphorylation as a genotoxicity endpoint. *Mutat. Res., Genet. Toxicol. Environ. Mutagen.* 679, 50–58.
- (21) Staal, Y. C., Hebel, D. G., van Herwijnen, M. H., Gottschalk, R. W., van Schooten, F. J., and van Delft, J. H. (2007) Binary PAH mixtures cause additive or antagonistic effects on gene expression but synergistic effects on DNA adduct formation. *Carcinogenesis* 28, 2632–2640.
- (22) Edgar, R., Domrachev, M., and Lash, A. E. (2002) Gene Expression Omnibus: NCBI gene expression and hybridization array data repository. *Nucleic Acids Res.* 30, 207–210.
- (23) Ernst, J., and Bar-Joseph, Z. (2006) STEM: a tool for the analysis of short time series gene expression data. *BMC Bioinf.* 7, 191.
- (24) Briede, J. J., van Delft, J. M., de Kok, T. M., van Herwijnen, M. H., Maas, L. M., Gottschalk, R. W., and Kleinjans, J. C. (2010) Global gene expression analysis reveals differences in cellular responses to hydroxyl- and superoxide anion radical-induced oxidative stress in caco-2 cells. *Toxicol. Sci.* 114, 193–203.
- (25) Sies, H. (2015) Oxidative stress: a concept in redox biology and medicine. *Redox Biol.* 4, 180–183.
- (26) Hu, C. T., Wu, J. R., Cheng, C. C., Wang, S., Wang, H. T., Lee, M. C., Wang, L. J., Pan, S. M., Chang, T. Y., and Wu, W. S. (2011) Reactive oxygen species-mediated PKC and integrin signaling promotes tumor progression of human hepatoma HepG2. *Clin. Exp. Metastasis* 28, 851–863.
- (27) Jafari, M., Salehi, M., Ahmadi, S., Asgari, A., Abasnezhad, M., and Hajigholamali, M. (2012) The role of oxidative stress in diazinon-induced tissues toxicity in Wistar and Norway rats. *Toxicol. Mech. Methods* 22, 638–647.
- (28) Matsuo, K., Sasaki, E., Higuchi, S., Takai, S., Tsuneyama, K., Fukami, T., Nakajima, M., and Yokoi, T. (2014) Involvement of oxidative stress and immune- and inflammation-related factors in azathioprine-induced liver injury. *Toxicol. Lett.* 224, 215–224.
- (29) Ha, C., and Dassopoulos, T. (2010) Thiopurine therapy in inflammatory bowel disease. *Expert Rev. Gastroenterol. Hepatol.* 4, 575–588.
- (30) Mates, J. M., Segura, J. A., Alonso, F. J., and Marquez, J. (2010) Roles of dioxins and heavy metals in cancer and neurological diseases using ROS-mediated mechanisms. *Free Radical Biol. Med.* 49, 1328–1341.
- (31) Liu, G. H., Qu, J., and Shen, X. (2008) NF-kappaB/p65 antagonizes Nrf2-ARE pathway by depriving CBP from Nrf2 and facilitating recruitment of HDAC3 to MafK. *Biochim. Biophys. Acta, Mol. Cell Res.* 1783, 713–727.
- (32) Waters, M. D., Jackson, M., and Lea, I. (2010) Characterizing and predicting carcinogenicity and mode of action using conventional and toxicogenomics methods. *Mutat. Res., Rev. Mutat. Res.* 705, 184–200.

(33) Kakehashi, A., Wei, M., Fukushima, S., and Wanibuchi, H. (2013) Oxidative stress in the carcinogenicity of chemical carcinogens. *Cancers* 5, 1332–1354.

(34) Monda, M., Messina, M., Scognamiglio, I., Lombardi, A., Martin, G. A., Sperlongano, P., Porcelli, M., and Stiuso, P. (2014) Short-term diet and moderate exercise in young overweight men modulate cardiocyte and hepatocarcinoma survival by oxidative stress. *Oxid. Med. Cell. Longevity* 2014, 1–7.

(35) Caraglia, M., Giuberti, G., Marra, M., Addeo, R., Mantella, L., Murolo, M., Sperlongano, P., Vincenzi, B., Naviglio, S., Del Prete, S., Abbruzzese, A., and Stiuso, P. (2011) Oxidative stress and ERK1/2 phosphorylation as predictors of outcome in hepatocellular carcinoma patients treated with sorafenib plus octreotide LAR. *Cell Death Dis.* 2, e150.